

Supporting Materials:

Photon shot noise limits on optical detection of neuronal spikes and estimation of spike timing

Brian A. Wilt[†], James E. Fitzgerald[†], and Mark J. Schnitzer^{†,‡}

[†] *James H. Clark Center, Stanford University, Stanford, CA 94305*

[‡] *Howard Hughes Medical Institute, CNC Program, Stanford University, Stanford, CA 94305*

SECTION S1: CALCULATION OF THE LOG-LIKELIHOOD RATIOS FOR SPIKE DETECTION

Here we calculate the mean and variance of the distributions of $L(\mathbf{f})$, the log-likelihood ratio of the two hypotheses. $L(\mathbf{f})$ is given by

$$L(\mathbf{f}) = \sum_{n=1}^N f_n \log \frac{\bar{S}_n}{\bar{B}} - \sum_{n=1}^N (\bar{S}_n - \bar{B}), \quad (\text{S1})$$

a linear combination of the Poisson-distributed variables, f_n . We rewrite the log-likelihood ratio in terms of $s_n \equiv (A/F_0) \tau \nu (e^{1/(\tau \nu)} - 1) e^{-n/(\tau \nu)}$. Most calculations in this paper rely on taking series approximations in s_n and performing the summations to leading order. This approach is valid as long as $A < F_0$, since $\tau \nu (e^{1/(\tau \nu)} - 1) e^{-n/(\tau \nu)}$ is bounded above by 1 for $n \geq 1$, and the interval of convergence for the series expansion of $\log(1+x)$ is $-1 < x \leq 1$. The mean, μ , and variance, σ , of the distribution of $L(\mathbf{f})$ under the null hypothesis $H^{(0)}$ of no spike having occurred are given by

$$\begin{aligned} \mu_L^{(0)} &= \frac{F_0}{\nu} \sum_{n=1}^N \log(1 + s_n) - \frac{F_0}{\nu} \sum_{n=1}^N s_n \\ &= \frac{F_0}{\nu} \sum_{n=1}^N (-s_n^2/2 + \mathcal{O}(s_n^3)) \approx -\frac{1}{2} \frac{(A\tau)^2}{F_0/\nu} \tanh \frac{1}{2\tau\nu} (1 - e^{-2N/(\tau\nu)}) \end{aligned} \quad (\text{S2})$$

$$\left(\sigma_L^{(0)}\right)^2 = \frac{F_0}{\nu} \sum_{n=1}^N \log^2(1 + s_n) = \frac{F_0}{\nu} \sum_{n=1}^N (s_n^2 + \mathcal{O}(s_n^3)) \approx -2\mu_L^{(0)}. \quad (\text{S3})$$

The mean and variance of the distribution of $L(\mathbf{f})$ under the alternate hypothesis $H^{(1)}$ that a spike occurred are given by

$$\begin{aligned}\mu_L^{(1)} &= \frac{F_0}{\nu} \sum_{n=1}^N (1 + s_n) \log(1 + s_n) - \frac{F_0}{\nu} \sum_{n=1}^N s_n \\ &= \frac{F_0}{\nu} \sum_{n=1}^N (s_n^2/2 + \mathcal{O}(s_n^3)) \approx -\mu_L^{(0)}\end{aligned}\quad (\text{S4})$$

$$\left(\sigma_L^{(1)}\right)^2 = \frac{F_0}{\nu} \sum_{n=1}^N (1 + s_n) \log^2(1 + s_n) = \frac{F_0}{\nu} \sum_{n=1}^N (s_n^2 + \mathcal{O}(s_n^4)) \approx -2\mu_L^{(0)}.\quad (\text{S5})$$

Thus, d' is given by

$$d' = \left(\mu_L^{(1)} - \mu_L^{(0)}\right) / \sigma_L \approx \sqrt{\frac{(A\tau)^2}{F_0/\nu} \tanh \frac{1}{2\tau\nu} (1 - e^{-2N/(\tau\nu)})} \approx \sqrt{\frac{(A\tau)^2}{F_0/\nu} \tanh \frac{1}{2\tau\nu}}.\quad (\text{S6})$$

To second order in s_n , the variances are the same, $\sigma_L^{(0)} \approx \sigma_L^{(1)}$.

Since $\Delta F/F$ is given by

$$\Delta F/F = (A/F_0) \tau\nu (1 - e^{-1/(\tau\nu)}),\quad (\text{S7})$$

if we sample at a reasonable rate, $\tau\nu \gg 1$, then $\Delta F/F \approx A/F_0$, and thus

$$d' \approx \Delta F/F \sqrt{F_0\tau/2}.\quad (\text{S8})$$

To validate the approximation that $L(\mathbf{f})$ is Gaussian distributed, we examine the m th-order cumulants κ_m of the $L(\mathbf{f})$ distribution. The first two cumulants of all distributions are the mean and variance. For Gaussian distributions, higher-order cumulants are zero. To calculate the cumulants of $L(\mathbf{f})$ we employ characteristic functions. The characteristic functions for $L(\mathbf{f})$, $\varphi_L(t)$, are given

by

$$\begin{aligned}
\varphi_L(t | H^{(0)}) &= \exp \left[\sum_{n=1}^N \bar{B} \left(e^{it \log(\bar{S}_n/\bar{B})} - 1 \right) \right] \exp \left[-it \sum_{n=1}^N (\bar{S}_n - \bar{B}) \right] \\
&= \exp \left[\sum_{m=1}^{\infty} \left(\frac{(it)^m}{m!} \sum_{n=1}^N \left(\bar{B} \log^m \frac{\bar{S}_n}{\bar{B}} \right) \right) \right] \exp \left[-it \sum_{n=1}^N (\bar{S}_n - \bar{B}) \right] \\
&= \exp \left[\sum_{m=1}^{\infty} \left(\frac{(it)^m}{m!} \kappa_m^{(0)} \right) \right]
\end{aligned} \tag{S9}$$

and

$$\begin{aligned}
\varphi_L(t | H^{(1)}) &= \exp \left[\sum_{n=1}^N \bar{S}_n \left(e^{it \log(\bar{S}_n/\bar{B})} - 1 \right) \right] \exp \left[-it \sum_{n=1}^N (\bar{S}_n - \bar{B}) \right] \\
&= \exp \left[\sum_{m=1}^{\infty} \left(\frac{(it)^m}{m!} \sum_{n=1}^N \left(\bar{S}_n \log^m \frac{\bar{S}_n}{\bar{B}} \right) \right) \right] \exp \left[-it \sum_{n=1}^N (\bar{S}_n - \bar{B}) \right] \\
&= \exp \left[\sum_{m=1}^{\infty} \left(\frac{(it)^m}{m!} \kappa_m^{(1)} \right) \right]
\end{aligned} \tag{S10}$$

where $\kappa_m^{(0)}$ and $\kappa_m^{(1)}$ represent the m th cumulant of the log-likelihood ratio distribution under hypotheses $H^{(0)}$ and $H^{(1)}$, respectively. To leading order in A/F_0 , $\kappa_m^{(0)} \approx \kappa_m^{(1)}$ for $m > 1$. The cumulants for $m > 1$ are given by

$$\kappa_m = \frac{F_0}{\nu} \sum_{n=1}^N s_n^m \approx \frac{F_0}{\nu} \left(\frac{A}{F_0} \tau \nu \right)^m \frac{(e^{1/(\tau\nu)} - 1)^m}{e^{m/(\tau\nu)} - 1} (1 - e^{-mN/(\tau\nu)}) \tag{S11}$$

which decrease with increasing m since $A/F_0 < 1$. Assuming $mN \gg \tau\nu$, these cumulants can be used to compute the standardized moments of $L(\mathbf{f})$, given by $\kappa_m / (\kappa_2)^{m/2}$, as

$$\frac{\kappa_m}{(\kappa_2)^{m/2}} = \frac{1}{(F_0/\nu)^{(m/2)-1}} \frac{(e^{m/(\tau\nu)} - 1)^{m/2}}{e^{m/(\tau\nu)} - 1}. \tag{S12}$$

For example, this allows us to compute the skew and excess kurtosis of $L(\mathbf{f})$. For $\tau\nu > 1$, they are approximately given by

$$\text{skew}(L(\mathbf{f})) \equiv \frac{\kappa_3}{(\kappa_2)^{3/2}} \approx \frac{2\sqrt{2}}{3} \frac{1}{\sqrt{F_0} \tau} \quad \text{excess kurtosis}(L(\mathbf{f})) \equiv \frac{\kappa_4}{(\kappa_2)^{4/2}} \approx \frac{1}{F_0 \tau}. \tag{S13}$$

The skew and excess kurtosis both approach 0 as the number of background photons collected over one time period increases. Thus, as long as the total number of photons collected over the duration, $\sim \tau$, of the signal waveform remains large, the Gaussian approximation used in our analytic treatment remains valid.

SECTION S2: RECEIVER OPERATING CHARACTERISTICS

When the total number of collected photons is large, we can approximate the distribution of $L(\mathbf{f})$ under hypothesis $H^{(j)}$ with a Gaussian distribution. This is a standard approximation to the Poisson distribution when the mean is large.

$$p_L(x | H^{(j)}) \approx \mathcal{N}\left(\mu_L^{(j)}, \left(\sigma_L^{(j)}\right)^2\right). \quad (\text{S14})$$

Here $p_L(x | H^{(j)})$ denotes the probability density of log-likelihood ratios of value x under hypothesis $H^{(j)}$ and $\mathcal{N}(\mu, \sigma^2)$ is a Gaussian distribution of mean μ and variance σ^2 (Fig. 1 A; section S1 in Supporting Material). Thus, the spike detection probability, P_D , is

$$\begin{aligned} P_D \equiv P(L(\mathbf{f}) > \log C | H^{(1)}) &= \frac{1}{\sqrt{2\pi}\sigma_L^{(1)}} \int_{\log C}^{\infty} \exp\left[-\frac{(x - \mu_L^{(1)})^2}{2(\sigma_L^{(1)})^2}\right] dx \\ &= 1 - \Phi\left[\frac{\log C - \mu_L^{(1)}}{\sigma_L^{(1)}}\right] \end{aligned} \quad (\text{S15})$$

where $\Phi(z)$ is the cumulative distribution function (CDF) of a standard Gaussian distribution. The Gaussian CDF can be written in terms of the error function, $\text{erf}(x)$, as

$$\Phi(z) = \frac{1}{2} \left[1 + \text{erf}\left(\frac{z - \mu}{\sqrt{2}\sigma}\right) \right]. \quad (\text{S16})$$

Similarly, the false positive probability P_F is given by

$$P_F \equiv P(L(\mathbf{f}) > \log C | H^{(0)}) = 1 - \Phi\left[\frac{\log C - \mu_L^{(0)}}{\sigma_L^{(0)}}\right]. \quad (\text{S17})$$

We can write P_D as a function of P_F ,

$$P_D = 1 - \Phi\left[\frac{\sigma_L^{(0)}}{\sigma_L^{(1)}} \Phi^{-1}(1 - P_F) - \frac{\mu_L^{(1)} - \mu_L^{(0)}}{\sigma_L^{(1)}}\right], \quad (\text{S18})$$

which defines the receiver-operating characteristic.

SECTION S3: SPIKE DETECTION WITH INTERFRAME SPIKING AND SUB-SAMPLING

We next compute how a change to the timing of the spike with respect to the beginning of a detector integration period affects spike detectability. We refer to this as an 'interframe spike.' Simultaneously, we also compute how a change to integration period, which we initially assumed to be $1/\nu$ (but could easily be less), affects spike detectability. We refer to this as 'sub-sampling.' To compute these effects, we add two new parameters to our initial model: a spike time parameter, $0 \leq t_0 \leq 1/\nu$, and an integration period, $0 < \varphi \leq 1/\nu$, which also could be interpreted as dwell time. Our new signal model is given by

$$T(t) = F_0 + Ae^{-(t-t_0)/\tau}\theta(t-t_0). \quad (\text{S19})$$

We integrate $T(t)$ with respect to time to determine the discrete signal, $\bar{T}_n^{(t_0)}$,

$$\bar{T}_n^{(t_0)} = \int_{n/\nu-\varphi}^{n/\nu} T(t) dt = \begin{cases} F_0\varphi + A\tau(1 - e^{-1/(\tau\nu)+t_0/\tau}) & \text{for } t_0 > n/\nu - \varphi \\ F_0\varphi + A\tau(e^{\varphi/\tau} - 1)e^{-n/(\tau\nu)+t_0/\tau} & \text{for } t_0 < n/\nu - \varphi \end{cases}. \quad (\text{S20})$$

The corresponding log-likelihood ratio is thus

$$L_T(\mathbf{f}) = \sum_{n=1}^N f_n \log \frac{\bar{T}_n^{(t_0)}}{\bar{B}} - \sum_{n=1}^N (\bar{T}_n^{(t_0)} - \bar{B}). \quad (\text{S21})$$

We have two cases to examine, depending on whether the spike takes place during an integration time or not. In the case that $t_0 < 1/\nu - \varphi$, the mean of the log-likelihood ratio under the null hypothesis is given by

$$\mu_{L_T}^{(0)} \approx -\frac{1}{4} \frac{(A\tau)^2}{F_0\varphi} e^{2t_0/\tau} (e^{\varphi/\tau} - 1)^2 \left(\coth \frac{1}{\tau\nu} - 1 \right), \quad (\text{S22})$$

whereas in the case that $t_0 > 1/\nu - \varphi$, we have

$$\mu_{L_T}^{(0)} \approx -\frac{1}{2} \frac{(A\tau)^2}{F_0\varphi} \left((e^{-1/(\tau\nu)+t_0/\tau} - 1)^2 + \frac{1}{2} e^{-2/(\tau\nu)+2t_0/\tau} (e^{\varphi/\tau} - 1)^2 \left(\coth \frac{1}{\tau\nu} - 1 \right) \right). \quad (\text{S23})$$

In both cases,

$$\left(\sigma_{L_T}^{(0)} \right)^2 \approx -2\mu_{L_T}^{(0)} \quad \mu_{L_T}^{(1)} \approx -\mu_{L_T}^{(0)} \quad \left(\sigma_{L_T}^{(1)} \right)^2 \approx -2\mu_{L_T}^{(0)}. \quad (\text{S24})$$

The time of the spike, t_0 , is uniformly distributed between 0 and $1/\nu$. We average over this random parameter by mixing the log-likelihood ratio distributions. Although the underlying model is no longer strictly Gaussian, we can find a heuristic figure-of-merit, \tilde{d}' , by taking the average $\mu_{L_T}^{(0)}$ over t_0 ,

$$\tilde{d}'_T \approx \sqrt{\frac{(A\tau)^2}{F_0/\nu}} \sqrt{1 + \frac{e^{-\varphi/\tau} - 1}{\varphi/\tau}}. \quad (\text{S25})$$

SECTION S4: SPIKE DETECTION WITH MISESTIMATED PARAMETERS

Initially, we assumed that we had perfectly estimated the fluorescence parameters. However, if we misestimate A as A' and τ as τ' , such that our expected signal $\bar{S} \rightarrow \bar{S}'$, then the new log-likelihood ratio $L_{S'}$ is given by

$$L_{S'}(\mathbf{f}) = \sum_{n=1}^N f_n \log \frac{\bar{S}'_n}{\bar{B}} - \sum_{n=1}^N (\bar{S}'_n - \bar{B}) \quad (\text{S26})$$

$$\mu_{L_{S'}}^{(1)} - \mu_{L_{S'}}^{(0)} \approx \frac{A\tau A'\tau'}{F_0/\nu} \frac{2}{\coth \frac{1}{2\tau\nu} + \coth \frac{1}{2\tau'\nu}} \left(1 - e^{-N/(\tau\nu) - N/(\tau'\nu)}\right) \quad (\text{S27})$$

$$\left(\sigma_{L_{S'}}^{(0)}\right)^2 \approx \left(\sigma_{L_{S'}}^{(1)}\right)^2 \approx \frac{(A'\tau')^2}{F_0/\nu} \tanh \frac{1}{2\tau'\nu} \left(1 - e^{-2N/(\tau'\nu)}\right) \quad (\text{S28})$$

Thus,

$$d'_{S'} \approx \sqrt{\frac{(A\tau)^2}{F_0/\nu} \frac{4/\tanh \frac{1}{2\tau'\nu}}{\left(\coth \frac{1}{2\tau\nu} + \coth \frac{1}{2\tau'\nu}\right)^2}}, \quad (\text{S29})$$

showing that, to leading order, misestimating the magnitude of the transient A does not affect our ability to discriminate spikes. To see the dependence on misestimation of τ more clearly, we expand this expression around $\tau - \tau'$. By assuming $\tau\nu > 1$, we find

$$d'_{S'} \approx d' \sqrt{1 - \frac{1}{4\tau^2\nu^2} \text{csch}^2 \frac{1}{\tau\nu} (1 - \tau'/\tau)^2} \approx d' \sqrt{1 - (1 - \tau'/\tau)^2/4}, \quad (\text{S30})$$

which shows that even large misestimations of τ have limited effect on the ability to detect spikes. However, the ability to discriminate spikes with misestimated parameters is always worse than the ability using the correct parameters since $d'_{S'}/d' < 1$ for all τ' .

SECTION S5: SPIKE DETECTION WITH A FINITE INDICATOR ON-TIME

In response to an external stimulus, optical indicators typically have a brief “on-time”, τ_{on} . We thus employ a signal model, $U(t)$, analogous to the previous $S(t)$:

$$U(t) = F_0 + A (1 - e^{-t/\tau_{on}}) e^{-t/\tau} \theta(t). \quad (\text{S31})$$

Integrating with respect to time yields \bar{U}_n , which is analogous to the previous \bar{S}_n :

$$\bar{U}_n = F_0/\nu + A \left[\tau (e^{1/(\tau\nu)} - 1) e^{-n/(\tau\nu)} - \tau_{eff} (e^{1/(\tau_{eff}\nu)} - 1) e^{-n/(\tau_{eff}\nu)} \right], \quad (\text{S32})$$

where

$$\tau_{eff} = \frac{\tau\tau_{on}}{\tau + \tau_{on}}. \quad (\text{S33})$$

The log-likelihood ratio is given by

$$L_U(\mathbf{f}) = \sum_{n=1}^N f_n \log \frac{\bar{U}_n}{\bar{B}} - \sum_{n=1}^N (\bar{U}_n - \bar{B}), \quad (\text{S34})$$

which has a mean given by

$$\begin{aligned} \mu_{LU}^{(0)} \approx & -\frac{1}{2} \frac{A^2}{F_0/\nu} \left[\tau^2 \tanh \frac{1}{2\tau\nu} (1 - e^{-2N/(\tau\nu)}) + \tau_{eff}^2 \tanh \frac{1}{2\tau_{eff}\nu} (1 - e^{-2N/(\tau_{eff}\nu)}) \right. \\ & \left. - 4\tau\tau_{eff} \frac{1 - e^{-N(\tau+\tau_{eff})/(\tau\tau_{eff}\nu)}}{\coth \frac{1}{2\tau\nu} + \coth \frac{1}{2\tau_{eff}\nu}} \right]. \end{aligned} \quad (\text{S35})$$

Collecting terms, we have

$$\mu_{LU}^{(0)} \approx -\frac{1}{2} \frac{(A\tau)^2}{F_0/\nu} \tanh \frac{1}{2\tau\nu} \left(1 - \frac{4\tau_{eff}/\tau}{1 + \tanh \frac{1}{2\tau\nu} \coth \frac{1}{2\tau_{eff}\nu}} + \frac{\tau_{eff}^2}{\tau^2} \tanh \frac{1}{2\tau_{eff}\nu} \coth \frac{1}{2\tau\nu} \right) \quad (\text{S36})$$

$$\left(\sigma_{LU}^{(0)} \right)^2 \approx -2\mu_{LU}^{(0)} \quad \mu_{LU}^{(1)} \approx -\mu_{LU}^{(0)} \quad \left(\sigma_{LU}^{(1)} \right)^2 \approx -2\mu_{LU}^{(0)}. \quad (\text{S37})$$

Thus, our final measure of spike detectability is given by

$$d'_U \approx d' \sqrt{1 - \frac{4\tau_{eff}/\tau}{1 + \tanh \frac{1}{2\tau\nu} \coth \frac{1}{2\tau_{eff}\nu}} + \frac{\tau_{eff}^2}{\tau^2} \tanh \frac{1}{2\tau_{eff}\nu} \coth \frac{1}{2\tau\nu}}, \quad (\text{S38})$$

which reduces to the original d' in the case that $t_{on} \rightarrow 0$. In the case that $\tau\nu \gg 1$, d'_U is approximately

$$d'_U \approx d' \left(1 - 3(\tau_{eff}/\tau)/2 + 7(\tau_{eff}/\tau)^2/8 + \dots \right). \quad (\text{S39})$$

These effects are illustrated in Fig. S1.

SECTION S6: CORRELATIONS BETWEEN CHANNELS IN FRET INDICATORS

Denote the number of photons detected in the donor channel as X and in the acceptor channel as Y . Denote the number of absorption events as N , a Poisson-distributed variable with mean \bar{N} . Index the excitation events as $j = 1, \dots, N$, such that x_j and y_j are binary variables indicating whether or not there was a photon emission from the donor or acceptor channels, respectively, for the j^{th} event. The possible outcomes are governed by a multinomial distribution

$$\begin{aligned} P(x_j = 1, y_j = 0) &= p \\ P(x_j = 0, y_j = 1) &= q \\ P(x_j = 0, y_j = 0) &= 1 - p - q \\ P(x_j = 1, y_j = 1) &= 0, \end{aligned} \quad (\text{S40})$$

where $P(x_j = 1, y_j = 0)$ and $P(x_j = 0, y_j = 1)$ represent the probability of donor and acceptor emission, respectively, $P(x_j = 0, y_j = 0)$ represents the probability of non-radiative decay. $P(x_j = 1, y_j = 1) = 0$, since a single excitation event cannot yield concurrent emissions in both channels. The total number of photons detected in each channel is

$$X = \sum_{j=1}^N x_j, \quad Y = \sum_{j=1}^N y_j. \quad (\text{S41})$$

This calculation does not include independent excitation of the acceptor channel, which typically occurs with only <15% of the frequency of donor excitation. We want to evaluate the covariance of the two channels. As a first step we calculate (with bracketed variables indicating the random

variables we are averaging over),

$$\langle XY \rangle_{\{N\},\{x,y\}} = \left\langle \sum_{j=1}^N x_j \sum_{k=1}^N y_k \right\rangle_{\{N\},\{x,y\}} \quad (\text{S42})$$

$$= \left\langle \sum_{j=1}^N \langle x_j y_j \rangle_{\{x,y\}|\{N\}} + \sum_{j \neq k} \langle x_j y_k \rangle_{\{x,y\}|\{N\}} \right\rangle_{\{N\}} \quad (\text{S43})$$

$$= pq \langle N(N-1) \rangle_{\{N\}} \quad (\text{S44})$$

$$= pq \bar{N}^2. \quad (\text{S45})$$

Note that this is different than a multinomial distribution with *fixed* N because for Poisson distributed N , $\langle N(N-1) \rangle = \bar{N}^2$, while for fixed $N = \bar{N}$ no averaging is needed and $\langle N(N-1) \rangle = N^2 - N$. On the other hand, the single channel averages are $\langle X \rangle = p\bar{N}$ and $\langle Y \rangle = q\bar{N}$. Thus, we obtain,

$$\text{Cov}(X, Y) = \langle XY \rangle - \langle X \rangle \langle Y \rangle = 0, \quad (\text{S46})$$

showing that the correlation between the two channels disappears entirely. The interpretation is that the anticorrelation due to the mutually exclusive nature of the multinomial statistics is canceled by the positive correlation due to the random fluctuations from absorption.

SECTION S7: RATIOMETRIC PROBES

Ratiometric indicators are used with two readout channels to infer the presence of spikes. Traditionally, these measurements are combined into a single trace of the ratio between the two channels, which then becomes the argument to the spike detection algorithm. For such a ratiometric analysis, we posit that we have two channels each approximately Gaussian distributed, $X \sim \mathcal{N}(\lambda_x, \lambda_x)$ and $Y \sim \mathcal{N}(\lambda_y, \lambda_y)$. We define their ratio $Z = X/Y$, guess that its mean is $\bar{Z} \sim \lambda_x/\lambda_y$, and note that near \bar{Z} fluctuations add in quadrature,

$$\frac{\sigma_z^2}{\bar{z}^2} = \frac{\sigma_x^2}{\bar{x}^2} + \frac{\sigma_y^2}{\bar{y}^2} \quad (\text{S47})$$

implying that

$$\sigma_z^2 = \left(\frac{\lambda_x}{\lambda_y} \right)^2 \frac{\lambda_x + \lambda_y}{\lambda_x \lambda_y}. \quad (\text{S48})$$

Thus, we hypothesize that

$$p_Z(z) \approx \mathcal{N} \left(\frac{\lambda_x}{\lambda_y}, \left(\frac{\lambda_x}{\lambda_y} \right)^2 \frac{\lambda_x + \lambda_y}{\lambda_x \lambda_y} \right) \quad (\text{S49})$$

and note that if $\lambda_y \gg 1$ (as required by the Gaussian approximation to Poisson noise statistics), this approximation works well empirically. With the ratiometric approach, we have

$$(\Delta\mu_{L_V})_n = \frac{F_0^{(1)} \left[1 + \left(A^{(1)}/F_0^{(1)} \right) \tau\nu \left(e^{1/(\tau\nu)} - 1 \right) e^{-n/(\tau\nu)} \right]}{F_0^{(2)} \left[1 + \left(A^{(2)}/F_0^{(2)} \right) \tau\nu \left(e^{1/(\tau\nu)} - 1 \right) e^{-n/(\tau\nu)} \right]} - \frac{F_0^{(1)}}{F_0^{(2)}} \quad (\text{S50})$$

$$\sigma_{L_V}^2 = \left(\frac{F_0^{(1)}}{F_0^{(2)}} \right)^2 \frac{F_0^{(1)} + F_0^{(2)}}{F_0^{(1)} F_0^{(2)}} \nu \quad (\text{S51})$$

$$d_V^2 = \sum_{n=1}^N (\Delta\mu_{L_V})_n^2 / \sigma_{L_V}^2 \approx \frac{F_0^{(1)} F_0^{(2)}}{F_0^{(1)} + F_0^{(2)}} \left(\frac{A^{(1)}}{F_0^{(1)}} - \frac{A^{(2)}}{F_0^{(2)}} \right)^2 \tau^2 \nu \tanh \frac{1}{2\tau\nu}, \quad (\text{S52})$$

where either $A^{(1)}$ or $A^{(2)}$ is negative, since the fluorescence signals are anti-correlated in the two channels.

By performing a full statistical analysis of each channel separately, one can make optimal use of the dynamics and statistics of the signal for spike detection. In this case, $\Delta\mu$ consists of paired measurements. Formally, it is given by

$$\Delta\mu_{L_W} = \begin{pmatrix} A^{(1)}\tau \left(e^{1/(\tau\nu)} - 1 \right) e^{-1/(\tau\nu)} \\ A^{(2)}\tau \left(e^{1/(\tau\nu)} - 1 \right) e^{-1/(\tau\nu)} \\ A^{(1)}\tau \left(e^{1/(\tau\nu)} - 1 \right) e^{-2/(\tau\nu)} \\ A^{(2)}\tau \left(e^{1/(\tau\nu)} - 1 \right) e^{-2/(\tau\nu)} \\ \vdots \\ A^{(1)}\tau \left(e^{1/(\tau\nu)} - 1 \right) e^{-N/(\tau\nu)} \\ A^{(2)}\tau \left(e^{1/(\tau\nu)} - 1 \right) e^{-N/(\tau\nu)} \end{pmatrix} \quad (\text{S53})$$

and Σ_{L_W} is a diagonal $2N \times 2N$ matrix given by

$$\Sigma_{L_W} = \text{diag} \left(F_0^{(1)}/\nu, F_0^{(2)}/\nu, F_0^{(1)}/\nu, F_0^{(2)}/\nu, \dots, F_0^{(1)}/\nu, F_0^{(2)}/\nu \right). \quad (\text{S54})$$

Thus, d_W^2 is given by

$$d_W^2 = \Delta \boldsymbol{\mu}_{L_W}^T \boldsymbol{\Sigma}_{L_W}^{-1} \Delta \boldsymbol{\mu}_{L_W} = \left(\frac{(A^{(1)})^2}{F_0^{(1)}} + \frac{(A^{(2)})^2}{F_0^{(2)}} \right) \tau^2 \nu \tanh \frac{1}{2\tau\nu}. \quad (\text{S55})$$

We can prove that the separate channel treatment is superior to the ratiometric treatment by showing that the ratio between the d 's, d_V^2/d_W^2 , is never greater than 1:

$$\begin{aligned} \frac{d_V^2}{d_W^2} &= \frac{F_0^{(1)} F_0^{(2)}}{F_0^{(1)} + F_0^{(2)}} \left(\frac{A^{(1)}}{F_0^{(1)}} - \frac{A^{(2)}}{F_0^{(2)}} \right)^2 \bigg/ \left(\frac{(A^{(1)})^2}{F_0^{(1)}} + \frac{(A^{(2)})^2}{F_0^{(2)}} \right) \\ &= \frac{\left(A^{(2)} F_0^{(1)} \right)^2 - 2A^{(1)} A^{(2)} F_0^{(1)} F_0^{(2)} + \left(A^{(1)} F_0^{(2)} \right)^2}{\left(A^{(2)} F_0^{(1)} \right)^2 + \left((A^{(1)})^2 + (A^{(2)})^2 \right) F_0^{(1)} F_0^{(2)} + \left(A^{(1)} F_0^{(2)} \right)^2} \leq 1. \end{aligned} \quad (\text{S56})$$

Thus, the separate channel treatment is always at least as sensitive as the ratiometric treatment of spike detection. The two approaches are equally effective if the two transient photon fluxes are equal in magnitude, $A^{(1)} = -A^{(2)}$.

There is also a regime in which a single channel is more sensitive than the ratiometric analysis. To find this regime, we look for fluorescence parameters satisfying the condition

$$\frac{d_V^2}{d_1^2} = \frac{F_0^{(1)} F_0^{(2)}}{F_0^{(1)} + F_0^{(2)}} \left(\frac{A^{(1)}}{F_0^{(1)}} - \frac{A^{(2)}}{F_0^{(2)}} \right)^2 \bigg/ \frac{(A^{(1)})^2}{F_0^{(1)}} \leq 1. \quad (\text{S57})$$

This condition is satisfied when

$$d_2^2 \leq 2 \sqrt{\frac{F_0^{(2)}}{F_0^{(1)}}} d_1' d_2' + d_1'^2. \quad (\text{S58})$$

This identifies the regime in which the second channel's d_2' is so much smaller than d_1' that an algorithm that disregards these measurements would have better performance than an optimal ratiometric treatment.

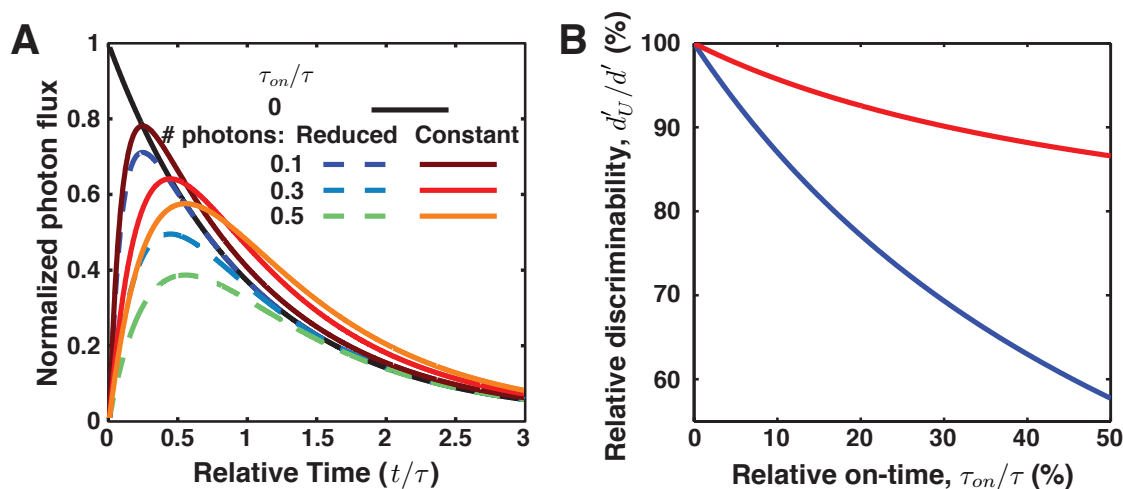


FIGURE S1. Spike detection using indicators with a finite on-time. Activity indicators require a time τ_{on} to respond to an action potential. (A) The time-varying photon emission rates during a signal from indicators with various on-times, $\tau_{on}/\tau = 0.1, 0.3,$ and 0.5 . The nonzero on-time reduces the number of photons emitted by the indicator (cool colors in dashed lines) relative to an idealized indicator with instantaneous on-time (black). However, even while holding constant the average number of photons collected from the indicator (warm colors in solid lines), spike detection suffers due to temporal broadening of the optical transient. (B) Relative effect on spike detectability, d'_U/d' , due to indicator on-time. The blue curve shows the effect of on-time for the case that the number of collected photons is reduced. The red curve shows the case in which the mean number of collected photons is held constant.